scientific reports

Check for updates

OPEN

High-content confocal analysis of tumorigenesis, cancer stem cells, and drug response in 3D cholangiocarcinoma cultures

Krittiyabhorn Kongtanawanich[1], Supawan Jamnongsong[1,2], Marianne Hokland[3], Methichit Wattanapanitch[4]✉ & Siwanon Jirawatnotai[1,2,5]✉

Three-dimensional (3D) culture models, particularly multi-spheroid models, are becoming increasingly essential in cancer drug discovery, particularly in stem cell and cancer stem cell (CSC) research. However, analytical methods for 3D multi-spheroid models, especially for single-cell and single-spheroid analysis in CSC research, remain limited. To address this gap we developed 3D multi-spheroid cholangiocarcinoma models that incorporate a CSC live-cell biosensor and a novel analysis method, 3D Surface Integrative Spheroid Profiling (3D-SiSP), utilizing high-content confocal imaging. 3D-SiSP quantifies spheroid area, allowing for both high- and low-throughput analyses. We demonstrate three key applications of 3D-SiSP. First, it outperformed traditional length-based methods for in vitro tumorigenesis measurements, offering greater precision. Second, 3D-SiSP enabled the calculation of individual spheroid areas along with real-time CSC biosensor signals, revealing larger spheroids had more undifferentiated cells. Lastly, 3D-SiSP facilitated simultaneous, real-time quantification of CSC content during anti-cancer drug testing in individual spheroids, providing evaluation of drug responses. Drug response differences across treatments were also quantified. Overall, 3D-SiSP provides a flexible and effective methodology for characterizing cancer cells and CSCs while evaluating anti-cancer drugs, applicable in both high- and low-throughput contexts. This approach enhances our understanding of CSC dynamics and supports the development of anti-CSC therapies.

Keywords Cholangiocarcinoma, Cancer stem cell, Live reporter, 3D multi-spheroid, 3D high-throughput drug screening, Image-based drug testing

Cell culture is a widely utilized in vitro model that enhances our understanding of cell biology, disease mechanisms, drug actions, and tissue engineering. Most research in cancer biology and drug responses has traditionally relied on two-dimensional (2D) cell cultures. However, these models have limitations in accurately mimicking physiological conditions and the complex tissue microenvironment. As a result, three-dimensional cultures, such as spheroids and organoids, have gained significant traction due to their superior ability to replicate physiological conditions[1]. 3D cell cultures have become particularly valuable in the realm of functional precision medicine, particularly for anti-cancer drug screening[2,3]. Furthermore, 3D cultures are extensively employed in cancer research, where structural complexity and the tumor microenvironment play crucial roles[4].

Studies focusing on clonal expansion and tumorigenesis in cancer stem cells can benefit from a multi-spheroid model[5–7]. This approach enables high-resolution analysis of individual cells across numerous spheroids. Unlike large spheroids that often develop necrotic cores and hinder high-resolution imaging or uniform stain penetration, our multi-spheroid model minimizes central cell death and provides consistent data at the single-cell level. Generating multiple spheroids simultaneously also boosts experimental throughput and statistical power, allowing robust analysis of clonal expansion and stem cell characteristics that are challenging to assess with single, large spheroids[6–9].

[1]Department of Pharmacology, Faculty of Medicine Siriraj Hospital, Mahidol University, Bangkok, Thailand. [2]Siriraj Center of Research Excellence for Precision Medicine and Systems Pharmacology, Faculty of Medicine Siriraj Hospital, Mahidol University, Bangkok, Thailand. [3]Department of Biomedicine, Aarhus University, Aarhus, Denmark. [4]Siriraj Center for Regenerative Medicine, Research Department, Faculty of Medicine Siriraj Hospital, Mahidol University, Bangkok, Thailand. [5]Faculty of Pharmacy, Silpakorn University, Nakhon Pathom, Thailand. ✉email: methichit.wat@mahidol.ac.th; siwanon.jir@mahidol.ac.th

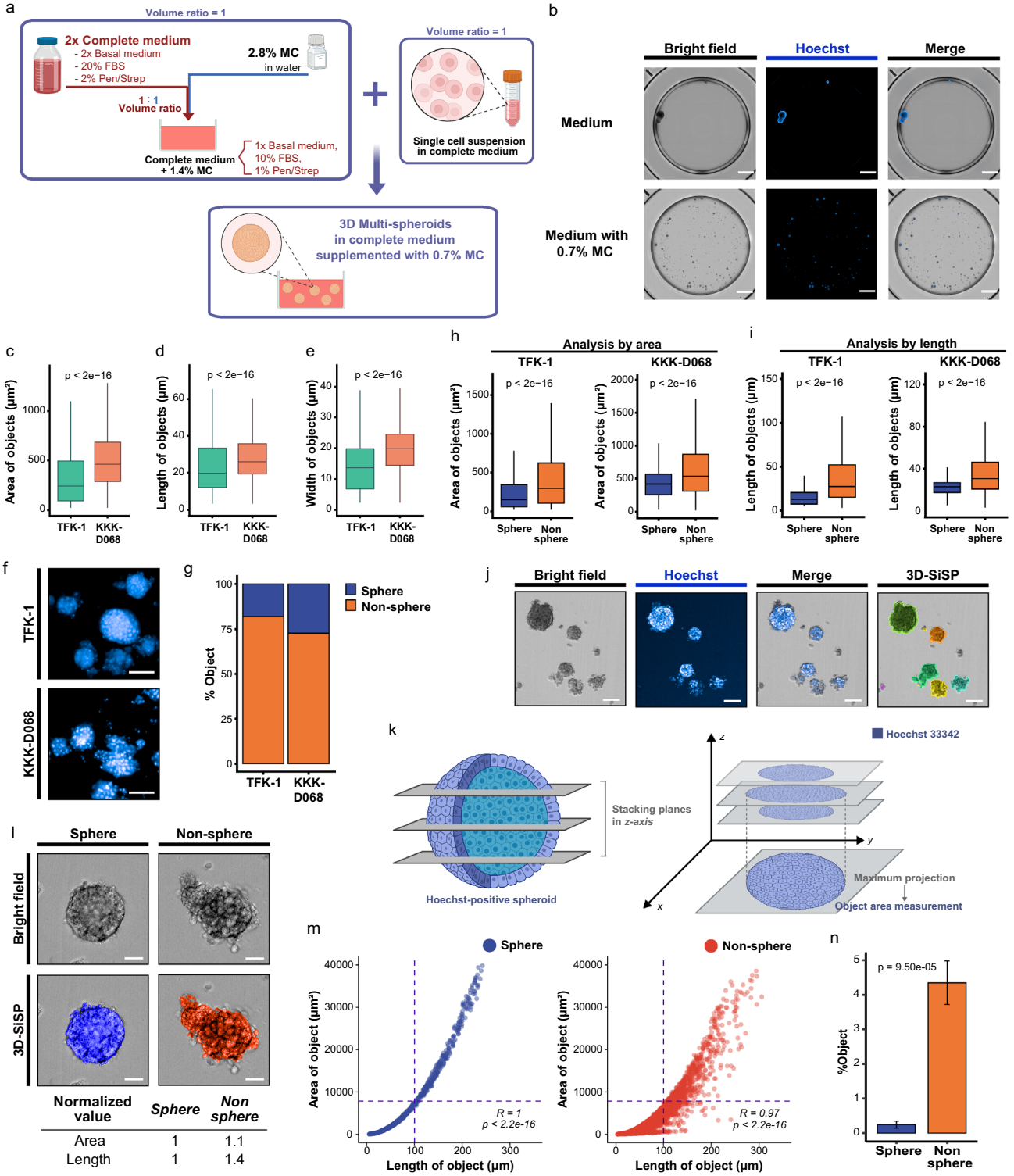

Despite their advances, the labor-intensive nature of 3D culture techniques and data analysis limits the development of these models for high-throughput drug testing. Currently, high-throughput 3D drug screening primarily relies on whole-well (bulk) metabolic and end-point assays, such as adenosine triphosphate (ATP) measurements[10,11]. However, this approach risks overlooking. This is particularly problematic when studying the dynamics of minor populations within 3D culture, such as stem cells or live biosensors as bulk and snapshot assays often fall short. To address these challenges, high-throughput imaging-based methods tailored for 3D cell culture models are ideal. One complication with spheroids and organoids is their propensity to form irregular shapes[12,13], which complicates the use of metrics like spheroid index (circularity) or length cut-offs[14,15], that may not yield fair comparisons. Therefore, methods capable of capturing single-cell information from live biosensors are highly desirable.

◀**Fig. 1**. The area-based analysis, 3D-SiSP, applies to both spherical and non-spherical spheroids. (**a**) 3D multi-spheroid model preparation (BioRender/Mahidol University). (**b**) Live-cell CSC biosensor TFK-1 spheroids (1000 cells/well) cultured for 14 days in ULA flat-bottomed trays with (lower) and without (upper) 0.7% MC in culture medium. Images are 9-field composites (5× objective); scale bar = 1 mm. (**c**–**e**) 3D multi-spheroid measurements for TFK-1 and KKK-D068 cells: (**c**) area, (**d**) length, and (**e**) width. (**f**) Morphology of TFK-1 and KKK-D068 multi-spheroids (20× objective, maximum projection, scale bar = 100 µm). Blue = nuclear area (Hoechst 33342). (**g**) Percentage of spherical vs. non-spherical objects in TFK-1 and KKK-D068 multi-spheroid cultures (single-object data, all seeding densities, n = 6 replicates/density). (**h**,**i**) Area-based (**h**) and length-based (**i**) size comparison of spherical vs. non-spherical objects in TFK-1 and KKK-D068. (**j**) Hoechst 33342-stained objects (500 cells/well) area analysis by 3D-SiSP (20× objective, maximum projection, scale bar = 100 µm). Right panel: 3D-SiSP nuclear area measurement. (**k**) 3D-SiSP image analysis schematic of 3D objects stained by Hoechst 33342 (BioRender/Mahidol University). (**l**) Spheroid area versus length variation example. Multi-color = 3D-SiSP nuclear area measurement. Area/length normalized to smallest values. (**m**) Scatter plots of spherical and non-spherical TFK-1 objects (n = 17,414) showing area vs. length distribution and correlation (R = Spearman, $p = p$ value). Spherical shape: width-to-length ratio 0.8–1.2 (n = 5909); non-spherical: others (n = 11,505). Dashed lines: area (7853.98 μm^2) and length (100 µm) cut-offs. (**n**) Bar graph: percentage of objects passing length but not area cut-off. (**m**,**n**) Object length/area data from maximum projection images. Box plots (**c**–**e**,**h**–**i**): single-object data, all seeding densities, n = 6 replicates/density, n = 21,865 (TFK-1), 16,778 (KKK-D068), Wilcoxon rank sum test. Bar graph (**n**): mean ± s.d., n = 6, t-test. Sphere: spherical objects, Non-sphere: non-spherical objects.

In this report, we present a novel high-throughput imaging-based technique designed to accommodate various spheroid shapes, including those containing CSC-specific biosensors. We demonstrate the effectiveness of these innovative approaches across several applications, including in vitro tumorigenesis, stem cell differentiation studies, and assessing anti-cancer drug efficacy in CSC-containing spheroids.

Results

Spheroid culture and measurement of 3D multi-spheroid model

3D-multi spheroid culture is commonly employed to investigate the growth of cancer cells and CSCs[4]. Typically, a limited number of the cells of interest are cultured in a serum-free medium supplemented with growth factors, using ultra-low attachment (ULA) flat-bottomed microplates to facilitate spheroid formation[16–18]. However, cell aggregation frequently complicates measurements and interpretations, particularly during high-throughput screening[19,20]. To reduce the impact of aggregation and optimize the spheroids suitable for high-throughput screening, we seeded TFK-1 cholangiocarcinoma (CCA) cells in 0.7% methyl cellulose (MC) using an easy-to-prepare method (detailed in the "Materials and methods" section) (Fig. 1a). MC increases the medium's viscosity, reduces cell–cell adhesion, thus allowing individual cells to self-assemble into distinct spheroids rather than clumping indiscriminately[21]. By adding MC to the culture medium, the position of each seeded cell is maintained, resulting in uniformly formed spheroids with minimal aggregation, in contrast to TFK-1 spheroids cultured in medium without MC (Fig. 1b).

Using this culture method, we evaluated the spheroid formations of TFK-1 and another CCA cell line, KKK-D068, by measuring the area, width, and length (please see detail in the "Materials and methods" section) of the spheroids formed. KKK-D068 exhibited a significantly larger total area, width, and length compared to the TFK-1 spheroids (Fig. 1c–e). Furthermore, both cell lines generated spheroids with both spherical and non-spherical (irregular) shapes, with only about 30% exhibiting spherical morphology (Fig. 1f,g). To further understand the disparities, we investigated the size differences between spherical and non-spherical spheroids. Notably, non-spherical spheroids displayed significantly larger dimensions, corroborating both the area and length measurements (Fig. 1h,i), suggesting that non-spherical spheroids may possess a greater growth potential than their spherical counterparts.

To account for these differences in the context of high-throughput drug screening, we developed a method based on area measurement to quantify spheroid growth in a compact multi-well format, termed 3D Surface Integrative Spheroid Profiling (3D-SiSP). This method involved initially labeling live cells with Hoechst 33342, a fluorescent nuclear stain. Subsequently, the area, width, and length of clusters of Hoechst-positive cells (spheroids) were measured (Fig. 1j). For comprehensive coverage of each spheroid, we combined 3–6 stacking planes into a single maximum projection image, preserving the highest fluorescent intensities of each position along the z-axis (Fig. 1k). This approach included objects with varying morphologies, both spherical and non-spherical (Fig. 1l). We proposed that utilizing object area derived from the maximum projection images provides a more accurate representation of 3D objects compared to traditional length-based methods[18,22,23]. In previous studies, it has been demonstrated that relying solely on length measurements can lead to misinterpretation[24]. As illustrated in Fig. 1l, applying both length-based and area-based (3D-SiSP) methods to spherical versus non-spherical objects, yielded comparable results for spherical objects (left), however, when both methods were applied to non-spherical objects (right), the length-based method resulted in a size overestimation of approximately 40% (1:1.4) compared to the area-based method (3D-SiSP).

We next examined the distribution of objects based on area and length, defining and illustrating the equivalent length and area cut-offs as the x and y intercepts for both spherical and non-spherical objects. Non-spherical objects exhibited scatter patterns that differed from those of spherical objects and were characterized by a higher proportion of objects that met the length cut-off but not the area cut-off (Fig. 1m,n). Consequently, relying solely on length measurements may lead to an overestimation of the sizes of non-spherical objects.

In contrast, when measuring spherical objects, the length-based measurements showed a high degree of correlation with the area-based 3D-SiSP method (Fig. 1m, sphere, R = 1). However, less correlation was observed when analyzing non-spherical objects, as the length-based measurements trended to overestimate their sizes (Fig. 1m, non-sphere, R = 0.97). Overall, the area-based 3D-SiSP method proved to be versatile, accommodating analyses of both spherical and non-spherical objects effectively.

Application of the 3D-SiSP for measuring in vitro tumorigenesis

In vitro tumorigenesis is commonly assessed in cancer research by measuring the number of spheroids that emerge from low-density cancer cell cultures. To demonstrate the application of the 3D-SiSP method in studying in vitro tumorigenesis, we utilized CCA cell lines containing the live-cell green fluorescence protein (GFP)-biosensor for CSCs (SORE6 reporter system)[23], which allows for the identification of the CSC population within the cancer cell culture by fluorescent microscopy. Cell lines containing GFP biosensor without SORE6 promoter (mCMV-dsCopGFP) were used as control[23]. This system is particularly useful for investigating the role of CSCs and their enrichment[23,25] (Fig. 2a). Live CSCs (GFP-positive (GFP^{POS})) and non-CSCs (GFP-negative (GFP^{NEG})) CCA cells can be enriched by Fluorescence-Activated Cell Sorting (FACS) (Fig. 2b).

The GFP^{POS} (CCA CSC) and GFP^{NEG} (CCA non-CSC) cells[25] were seeded at various densities (1000, 500, 250, 125, and 63 cell/well) in complete RPMI 1640 medium supplemented with 0.7% MC in an ULA flat-bottom 96-well plates, as illustrated in Fig. 2a. After 14 days of culture, the spheroids were stained with Hoechst 33342 before imaging the entire well to minimize selection bias. As previously reported[26–28], the GFP^{POS} CCA exhibited a higher spheroid formation potential, evident by the increased number of spheroids across different seeding densities (Fig. 2c). The raw images were analyzed in parallel using the length-based and 3D-SiSP methods to determine spheroid counts and object values. Typically, spheroid measurement relies on spheroid length with a defined cut-off[14,17,22]. In this study, we set the length cut-off at 100 µm[22,23], which is equivalent to an area of 7853.98 μm^2 for spheroids with a spherical shape. We then compared the results obtained from the 3D-SiSP method (Fig. 2d,e) with those from the length-based method (Fig. 2f,g).

As anticipated, we found that the GFP^{POS} CCA CSCs generated a significantly higher number of spheroids in 3D culture compared to their GFP^{NEG} counterparts, as measured by both methods (Fig. 2d–g). Notably, the 3D-SiSP method exhibited greater discriminative power than the length-based method, both in determining spheroid count and object values; it successfully detected significant differences in spheroid numbers at a seeding density of 250 cell/well, while the length-based method only achieved this at 500 cell/well, adhering to the cut-offs (100 µm for length-based, and 7853.98 μm^2 for 3D-SiSP) (Fig. 2d,f).

It has been shown that the smaller spheroids play important roles in drug screening and tumorigenesis[7,29]. Therefore, we also analyzed the spheroids without applying any cut-off (Fig. 2e,g). In this case, the mean object area or length was utilized (Fig. 2e,) as all values were biologically meaningful. Based on this analysis, the 3D-SiSP method proved to be more sensitive, successfully detecting significant differences in object values at the seeding of 125 cells/well (Fig. 2e), whereas the length-based method could only detect such differences at 500 cells/well (Fig. 2g).

Application of 3D-SiSP in cancer cells with GFP-based biosensor for CSCs

Since CSCs are highly plastic, real-time dynamic indicators such as live biosensors are essential tools for CSC research[4,30]. To apply the 3D-SiSP method in CSC studies, we utilized CCA cell lines previously established in our lab, which specifically express a short half-life version of GFP in CSCs (GFP^{POS})[23,25].

We examined the spontaneous differentiation of CCA CSCs in our 3D multi-spheroid culture model. The GFP^{POS} cells were sorted into highly pure populations (95.10%, Fig. 2b) and cultured as depicted in Fig. 1a. Imaging was conducted in both Hoechst 33342 and GFP channels on days 0 and 14 of the culture. On day 0, all sorted GFP^{POS} cells were present in the culture (Fig. 3a, top left), compared to the CCA control cells, containing an empty vector, mCMV (Fig. 3a, lower left). By day 14, the GFP^{POS} spheroids had increased in size (Fig. 3a, top right), consistent with CSC tendency to form larger and more complex spheroids[31]. We also observed inter-spheroid and intra-spheroid heterogeneity in the GFP signal within the 3D cultures (Fig. 3a, top right), indicating spontaneous loss of stemness (differentiation) over the 14 days of 3D culture. This supports the transient nature and complex roles of CSCs in cancer spheroids.

To measure the size of the 3D object for high-throughput application, we generated maximum projection images where spheroids were identified based on the Hoechst 33342 positive area, the highest GFP intensities of each position along the z-axis in the image (Fig. 3b). We then classified the differentiation status of the cancer spheroids into undifferentiated and differentiated based on the GFP intensity cut-off (Fig. 3c). Integrating 3D-SiSP measurements and GFP intensity revealed that undifferentiated spheroids exhibited a larger spheroid area compared to differentiated spheroids (Fig. 3d), indicating the superior spheroid forming capability of the GFP^{POS} cells. Furthermore, we also verify the stemness phenotype by investigating the co-expression of GFP and some established CCA CSCs surface proteins[32–34]. Both $CD44^+/CD133^+$ and $CD133^+/LGR5^+$ were highly expressed in the undifferentiation group, ensuring the stemness characteristics (Fig. 3e).

Application of 3D-SiSP for evaluating CSC content in anti-cancer drug testing

CSCs are believed to play a crucial role in driving drug resistance[35,36]. The 3D multi-spheroid culture system is a widely used technique for studying CSCs and their responses to anti-cancer drugs[17,37,38]. To investigate the role of CSCs under anti-cancer drug treatments, we developed a high-throughput image-based protocol for the 3D multi-spheroid culture to assess drug cytotoxicity and measure the CSC population in response to various drug doses (Fig. 4). We employed Calcein Blue AM and Zombie NIR™ to differentiate between live and dead cells, respectively. To ensure that no false positives of Calcein Blue AM from the dead populations and optimize concentrations and staining times for the 3D-SiSP method, the dead cells were separately stained

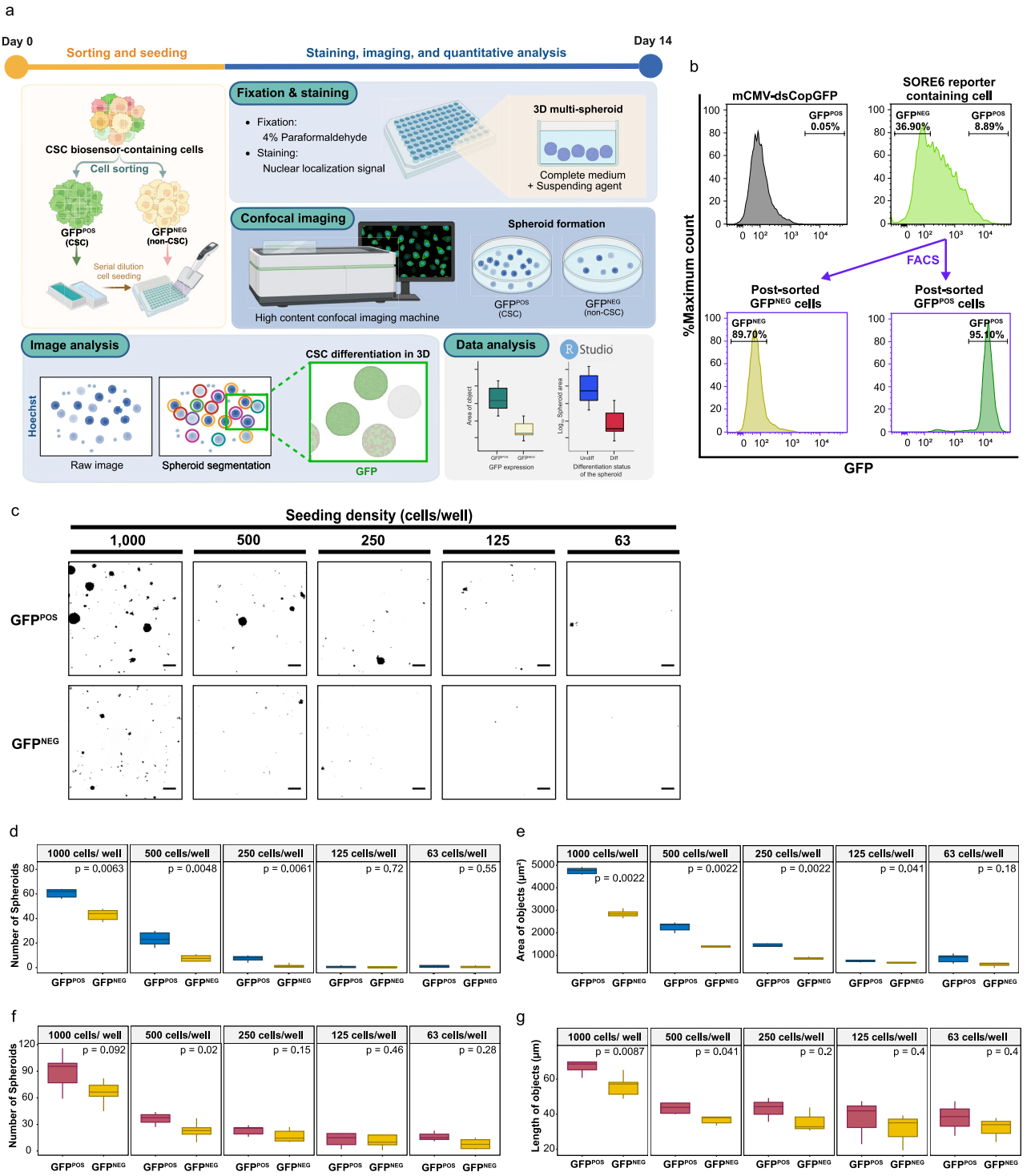

Fig. 2. Analysis of tumorigenesis potential of CCA CSC by the 3D-SiSP and traditional length-based method. (**a**) Schematic diagram of the in vitro tumorigenesis assessment by the 3D-SiSP. (Created by BioRender.com/Mahidol University). (**b**) Gating strategy for FACS. The CSC live-cell biosensor-containing TFK-1 cells were sorted into GFP^{POS} and GFP^{NEG} populations. (**c**) Representative images of Hoechst 33342-stained GFP^{POS} and GFP^{NEG} TFK-1 cells at indicated seeding densities. Scale bar = 300 µm. The images were taken using a 5× objective lens. (**d**,**f**) Quantitative analysis of the number of spheroids of GFP^{POS} and GFP^{NEG} populations. Area 7853.98 μm^2 (**d**) or length 100 µm (**f**) was used as a cut-off for spheroid determination. (**e**,**g**) Quantitative analysis of the object values. The results are area (**e**) and length (**g**) of Hoechst 33342-positive objects of GFP^{POS} and GFP^{NEG} populations. In (**d**)–(**g**), the data were from $n \geq 3$, and statistical significances were analyzed by the Wilcoxon rank sum test.

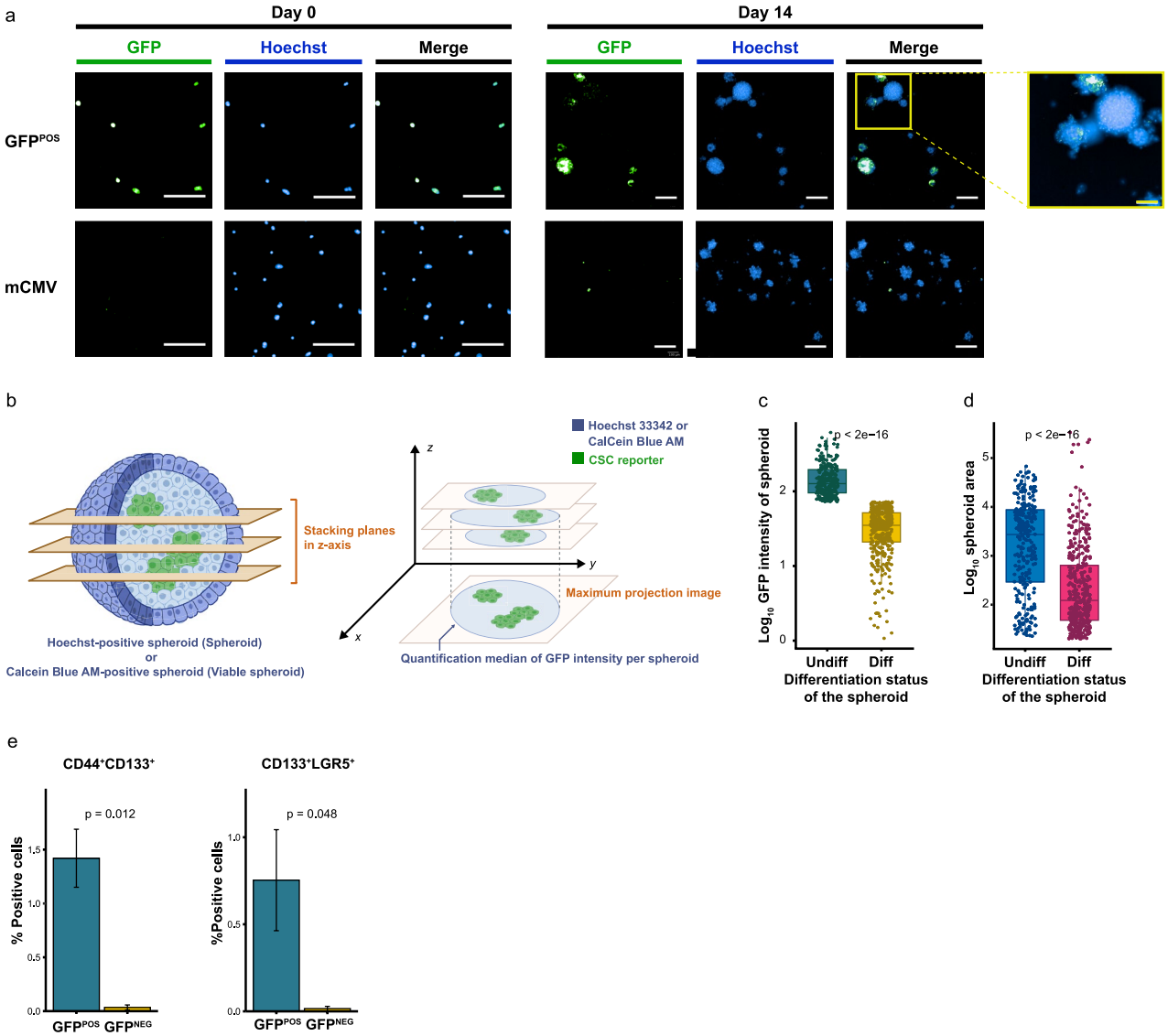

Fig. 3. Application of 3D-SiSP in CCA cells with the GFP-based live-cell biosensor for CSCs. (**a**) Spontaneous differentiation of the 3D multi-spheroids. GFP^{POS}CCA cells were seeded at 1000 cells/well and imaged on days 0 and 14, as indicated. Green = GFP-positive CSCs, blue = nuclear area of spheroids (Hoechst 33342), white scale bar = 200 µm, yellow scale bar = 100 µm. The images were captured using a 20× objective lens. (**b**) Schematic diagram of 3D-SiSP image analysis of live CSC content in the spheroids by Hoechst 33342 or Calcein Blue AM double staining (Created by BioRender.com/Mahidol University). (**c**,**d**) Quantitative analysis of the undifferentiated and differentiated 3D multi-spheroid on log_{10} spheroid GFP intensity (**c**) and log_{10} spheroid area (**d**). The data represent from n = 278 (undiff) and 490 (diff). Statistical significances were analyzed by the Wilcoxon rank-sum test. (**e**) Co-expression of $CD44^+/CD133^+$ (left) and $CD133^+/LGR5^+$ (right) protein surface markers of the GFP^{POS} and GFP^{NEG} populations analyzed by flow cytometry. The data represent mean ± s.d., n = 3.

with Zombie NIR™ before being added to the healthy spheroids. The viable spheroids were specifically stained at concentrations of 10 and 5 µM Calcein Blue AM, with no false positives from the dead population (positive for Zombie NIR™) (Fig. 5a). The 10 µM concentration exhibited a better foreground-to-background ratio and provided a longer-lasting stain compared to the 5 µM concentration. We subsequently optimized the incubation time for 10 µM Calcein Blue AM, adjusting it to a duration of 10–190 min (Fig. 5b). Based on these results, we will conduct further experiments utilizing staining durations between 10 and 70 min.

Next, we investigated the CSC-mediated response to anti-cancer drug treatments including 5-fluorouracil (5-FU) and gemcitabine in live biosensor-containing TFK-1 cells. As anticipated, the area of Calcein Blue AM positive cells was decreased in a dose-dependent manner, indicating increased cell death with higher drug doses.

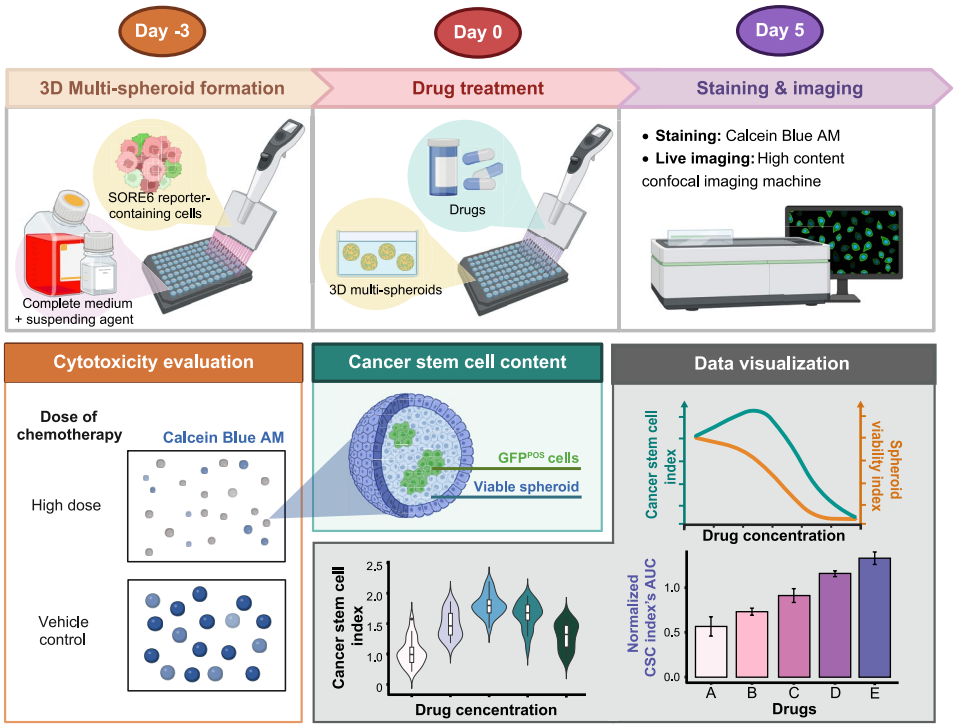

Fig. 4. Schematic diagram of the 3D multi-spheroid model for evaluating anti-cancer drugs in CCA CSCs (Created by BioRender.com/Mahidol University).

Interestingly, the GFP^{POS} area increased at certain doses of anti-cancer drugs compared to the control group (Fig. 5c).

We quantitatively analyzed spheroid viability and CSC content, as shown in Fig. 3b, resulting in the determination of the spheroid viability index (SVI) and CSC index (Fig. 5d,e). Analysis of the CSC index in individual spheroids revealed the highest CSC enrichment with 0.05 µM (4.7 $\log_{10}$ pM) of 5-FU, achieving a CSC index of 1.66 (Fig. 5d). Treatment with 0.01 µM (4 $\log_{10}$ pM) gemcitabine yielded a CSC index of 1.47 (Fig. 5e). The distribution of the CSC index for individual spheroids treated with 5-FU and gemcitabine is displayed in Fig. 5f and g, respectively. Furthermore, we examined the relationship between spheroid GFP intensity and spheroid area. The highest positive correlations between GFP intensity and spheroid area were observed at 0.05 µM of 5-FU and 0.01 µM of gemcitabine treatment (Fig. 5h,i), corresponding to the highest CSC indices (Fig. 5d–g).

To further compare CSC content in viable spheroids across treatments, we calculated the "Normalized CSC index's area under the curve (AUC)." This involved calculating the CSC index AUC of each treatment across a range of doses and normalizing it by the CSC index AUC of the vehicle control. The dose range was selected based on SVI, ensuring equivalent viability across conditions. The normalized CSC index's AUC for both 5-FU and gemcitabine, calculated within the SVI range of 0.6–1, indicated that both drugs can enhance CSC content within the tested dose ranges Notably 5-FU (AUC 1.18) exhibited significantly higher CSC content compared to gemcitabine (AUC 1.03) (Fig. 5j). These results suggest that CSCs are enriched under sublethal doses of chemotherapies, demonstrating distinct induction patterns.

Discussion

Three-dimensional multi-spheroids are increasingly utilized in cancer and stem cell research[39,40], including drug screening. Consequently, many researchers are turning to 3D cell culture models, such as spheroids and organoids, which better mimic in vivo conditions This shift highlights the need for the development of novel 3D platforms and analytical methods suited to these culture models[41]. While 3D multi-spheroids are typically expected to exhibit a spherical shape, studies have shown that, under certain conditions, they can adopt non-spherical morphologies. These morphologies can be influenced by factors such as the culture medium, extracellular matrix[42], the nature of the cells[43], and their heterogeneity[44–46].

In this study, we show that 3D multi-spheroids derived from CCA were predominantly non-spherical, necessitating analyses specifically designed to assess both spherical and non-spherical spheroids. In vitro tumorigenicity measurement using 3D multi-spheroids is typically conducted using a length-based method[16–18], which can lead to misinterpretations, particularly when dealing with non-spherical shapes[24].

Theoretically, the most informative 3D multi-spheroid growth evaluation should be analyzed based on spheroid volume, where both horizontal and vertical information are rendered into the 3D simulated spheroid for further spheroid volume calculation. However, the spheroid volume consumes high data processing and analysis, which is not suitable for high-throughput techniques. Herein, the 3D-SiSP method offers a solution

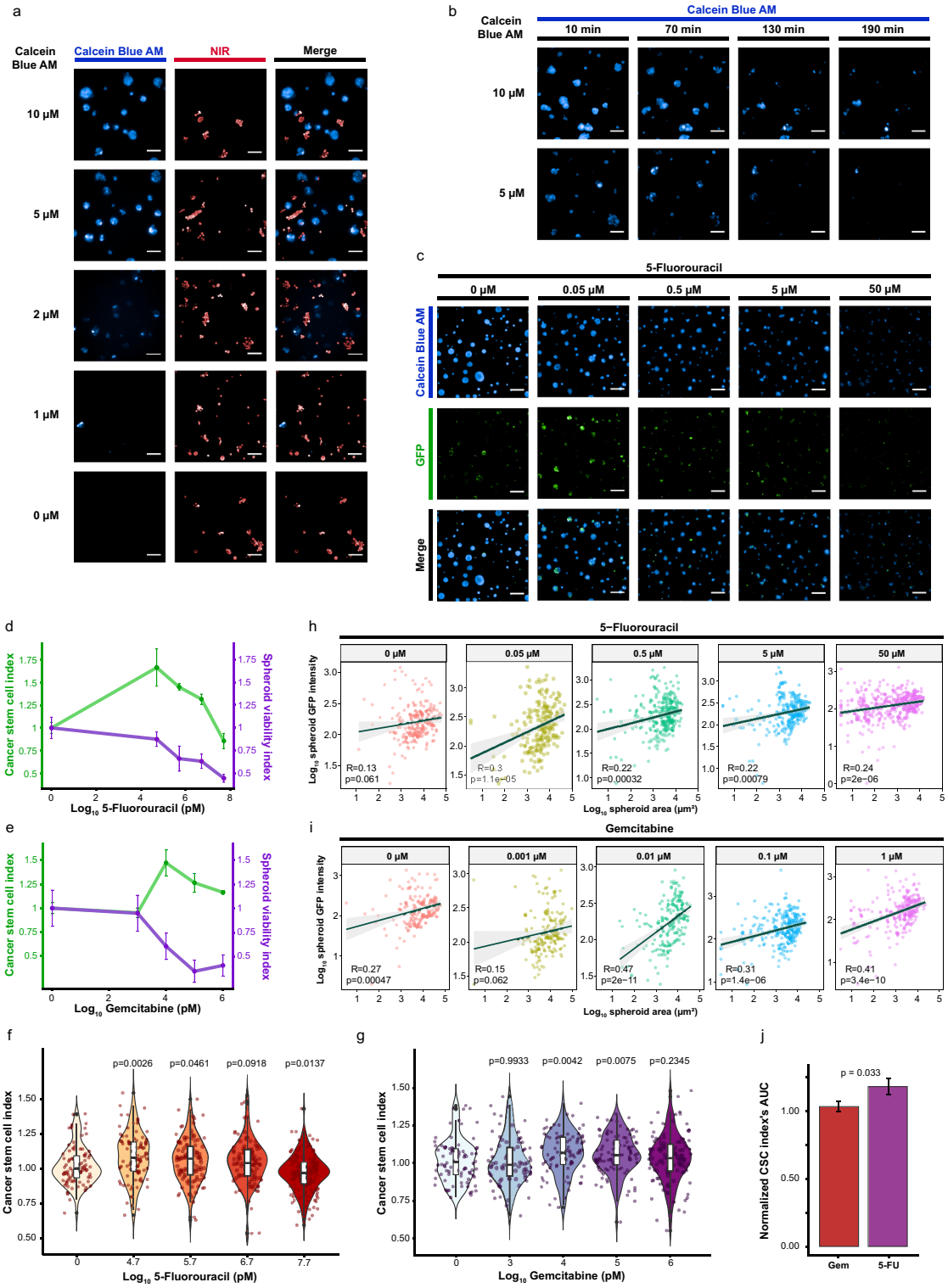

to this issue as it is based on area measurements rather than length, allowing for a more accurate and reliable assessment[47]. The number of z-stacking planes was optimized to balance high-throughput imaging efficiency with sufficient analytical resolution. In our experiments, we used the same number of imaging planes for each experiment and cell line-three imaging planes were used for the tumorigenic assay, and six imaging planes were used for the drug testing experiment to cover the whole spheroid. The drug testing experiment needs higher planes because the experiment started with a higher number of initial cell-seeding densities, resulting in bigger spheroid sizes.

The tumorigenic potential of cancer cells in 3D can be used to evaluate the growth of individual clones[48,49]. Instead of applying cell seeding density for interpretation, in vitro tumorigenicity measurement should be conducted under well-distributed culture conditions at very low seeding densities. The 3D-SiSP method appears particularly suitable for this purpose, as it can measure and analyze every spheroid produced in each 3D

◀**Fig. 5.**. 3D multi-spheroid model for evaluating CSC-mediated anti-cancer drug response. (**a**) Optimization of Calcein Blue AM concentrations. Dead cells stained by Zombie NIR (NIR) were included as a negative control. The images were taken 10 min after Calcein Blue AM incubation. (**b**) Calcein Blue AM retention from 10 to 190 min after staining. Doses of Calcein Blue AM are indicated on the left side. The images in (**a**) and (**b**) were taken using the 10× objective lens. Scale bar = 100 µm. (**c**) Calcein Blue AM stained viable spheroids across a range of 5-FU concentrations. Each image is composed of 6 fields from a 20× objective water lens. Scale bar = 300 µm. For all images, Blue = viable spheroids (Calcein Blue AM), Red = dead cells (Zombie NIR™), Green = GFP^{POS} (dsCopGFP). The double y-axis graph shows cytotoxicity evaluation of the 3D multi-spheroids under 5-FU (**d**) and gemcitabine (**e**) represented as SVI (right y-axis) and CSC index (left y-axis). The data represent mean ± s.d., n = 3. (**f**,**g**) Violin plots show the CSC index across a range of 5-FU (**f**) and gemcitabine (**g**) concentrations. Statistical significances were analyzed by the Wilcoxon rank-sum test by comparing each concentration and the vehicle control. (**h**,**i**) Scatter plots between Log_{10} spheroid area and Log_{10} GFP intensity of spheroids show correlations across a range of 5-FU (**h**) and gemcitabine (**i**) concentrations. The regression line (black line) was estimated by linear regression of Pearson correlation with a 95% confidence interval (gray band). R = Pearson correlation coefficient, $p = p$ value. In (**f**)–(**i**), the data represent single spheroid information ranging from 76 to 169. (**j**) Bar graphs show the normalized CSC index AUCs of the 3D multi-spheroids under 5-FU and gemcitabine in the dose range where SVI equals 0.6–1. The data represent mean ± s.d.; n = 3. Statistical significances were analyzed by t-test. *5-FU* 5-fluorouracil, *Gem* gemcitabine, *AUC* area under the curve, *SVI* spheroid viability index.

culture. This capability is especially valuable when analyzing highly heterogeneous cell populations, allowing for quantitative investigations into aspects of cancer biology, such as the differentiation of CSC-expressing spheroids and the crosstalk between CSCs and the tumor microenvironment. Overall, these findings suggest that the effectiveness of the 3D-SiSP method in this context should warrant extensive future testing.

To apply the 3D-SiSP method to the in vitro tumorigenic assay, we utilized the object area measurement to quantify the spheroids in the culture. This approach does not rely on subjective cut-off[14,17,22,23]. When combined with live/dead staining, it enables the exclusion of dead cells, ensuring that only viable spheroids are measured. Small spheroids and tumoroids are commonly used for high-throughput drug screening because their smaller size facilitates easier handling and manipulation, making them well-suited for large-scale studies. Therefore, they should not be excluded based on subjective cut-offs.

We demonstrated that the 3D-SiSP method, using object area measurement, is effective for analyzing small-sized spheroids. Both small and large spheroids offer unique advantages and applications in cancer research[6,7]. The choice between them depends on the specific goals and requirements of the study[50].

Interestingly, the 3D-SiSP method relies on maximum projection, which combines imaging planes into one. Ideally, the volume of spheroids should be assessed through 3D confocal imaging; however, this may be challenging in high throughput applications due to the time-consuming nature of the process and the substantial workload associated with data acquisition, storage, and analysis. Our system is also suitable for studying CSCs as it facilitates real-time identification and characterization of individual cells, including CSCs within the spheroids. Conventional whole-well and non-imaging-based assays may not capture these small populations effectively.

Evaluating the impact of anti-cancer drugs on CSCs is challenging, as these drugs often affect both cancer cells and CSCs. Providing more evidence of CSC biology with additional markers, such as other stemness-related markers, and dead staining dye would be used as a secondary validation to increase reliability and enhance the chance of biological discovery. Moreover, comparing the CSC content resulting from drugs with different killing efficiencies is difficult. Therefore, it is essential to use a dose or dose range that results in a comparable killing effect across treatments.

Taken together, we have demonstrated that the 3D-SiSP method is suitable for evaluating in vitro tumorigenicity, along with other CSC characteristics such as differentiation. Furthermore, this method is effective for assessing cytotoxicity and CSCs in the context of anti-cancer treatment. Additionally, the 3D-SiSP method may be flexible enough to be applied to other 3D culture models such as embryoid bodies and organoids in regenerative medicine. Altogether, our 3D-SiSP method, along with the three example applications, provides laboratory protocols and tutorial analysis code in R language and offers a comprehensive tool for high-throughput imaging and analysis in cancer and CSC research.

Materials and methods

The experimental protocols described in the peer-reviewed paper including the 3D Surface Integrative Spheroid Profiling (3D-SiSP) for evaluating in vitro tumorigenicity and CSC-mediated anti-cancer drug response, have been published on protocol.io (https://www.protocols.io/private/ECE27AC5049811EFBE540A58A9FEAC02).

Cell lines

The human CCA cell lines, TFK-1 and KKK-D068 were obtained from the Japanese Collection of Research Bioresources (JCRB, Osaka, Japan)[51]. TFK-1 cells were cultured in Roswell Park Memorial Institute 1640 Medium (RPMI 1640), KKK-D068 cells were cultured in Dulbecco's Modified Eagle's Medium (DMEM), and both media were supplemented with 10% fetal bovine serum (FBS) (Thermo Fisher Scientific), and 1% penicillin/streptomycin (Gibco). All cultures were maintained at 37 °C in a humidified 5% CO_2 atmosphere.

Preparation of biosensor-containing cells, sorted GFP^{POS}, and GFP^{NEG} cells

The six tandem repeats of the SOX2/OCT4 response element (SORE6) are used to drive a short half-life version of green fluorescence protein (dsCopGFP), while the minimal cytomegalovirus (mCMV) promoter is used to enhance the biosensor protein signal. The biosensor system (SORE6-mCMV-dsCopGFP) with its control construct (mCMV-dsCopGFP)[23] as lentiviral plasmids was a kind gift from Dr. Lalage M. Wakefield, NCI, USA. To construct the CCA biosensor-containing cells, the procedures including the generation and transduction of lentiviral biosensors were performed according to our previous work[25].

According to data published in[25], cells positive for the SORE6 biosensor (GFP^{POS}) are considered CSCs, while cells negative for the SORE6 biosensor (GFP^{NEG}) are considered non-CSCs. To purify GFP^{POS} and GFP^{NEG} cells, the biosensor-containing CCA cells were detached using 0.25% trypsin–EDTA, and then washed with phosphate-buffered saline (PBS) supplemented with 3% FBS. The cells were filtered through a cell strainer before being sorted two times on a BD FACS Aria™ III Cell Sorter to increase the purity. The sorted cells were kept on ice in the dark for no more than 2 h before seeding. The data were analyzed by FlowJo software (version 10.8.1) and the matched CCA cell line containing the mCMV-dsCopGFP construct was used as a gating control.

Culture optimization for 3D multi-spheroids

3D multi-spheroids were developed from CCA cells cultured according to the strategy shown in Fig. 1a. Briefly, StemXVivo MC (R/D Systems) was mixed with the culture media comprising either RPMI1640 for TKI-1 or DMDM for KKK-D068 supplemented with 10% FBS and 1% Pen/Strep (Complete Medium) to a final concentration of 1.4% before being plated onto a flat-bottomed 96-well ULA microplate (Corning). Finally, CCA single-cell suspension in complete medium was seeded onto the prepared plate at a ratio of 1:1 v/v, thus resulting in 0.7% MC final concentration for the 3D multi-spheroid cultures (Fig. 1a). Specific details of the in vitro tumorigenic assays and evaluation of CSC-mediated anti-cancer drug response using 3D multi-spheroids are provided in the "Tumorigenic assay" to "CSC-mediated anti-cancer drug response" sections.

Immunofluorescent staining and flow cytometry

Biosensor-containing TFK-1 cells were double-stained for the detection of CD44/CD133 or CD133/LGR5 protein surface markers as previously described[25]. Briefly, cells were washed with 3% FBS in PBS and subsequently blocked with Odyssey blocking buffer (Li-Cor) for 30 min on ice. Following blocking, cells were incubated for 15 min in the dark with an antibody cocktail containing: PE anti-human CD133 (mouse, #372803, BioLegend), PerCP-Cy5.5 anti-mouse/human CD44 (rat, #103031, BioLegend), and APC anti-human LGR5 (rat, #130-100-85, Miltenyi Biotec). Live/Dead Zombie NIR was included in the cocktail to assess cell viability. Isotype-matched antibodies served as controls for non-specific binding. TFK-1 cell lines transduced with mCMV-dsCopGFP served as controls for GFP expression. Stained cells were analyzed on a BD LSR Fortessa™ Cell Analyzer (BD Biosciences). Flow cytometry data were analyzed using FlowJo software (version 10.8.1).

High-content confocal imaging

The high-throughput screening (HTS) microplate reader Operetta CLS™ (PerkinElmer) was utilized for high-content confocal imaging at magnifications 5× and 20× magnification. Confocal images were captured in bright field, GFP, Hoechst 33342, near-infrared (NIR), and Calcein Blue AM channels depending on the specific settings for each experiment, covering 3 or 6 z-planes (3 planes for the tumorigenic assay and 6 planes for CSC-mediated anti-cancer drug response) to encompass the entire spheroid. All fields from the entire culture were imaged for the in vitro tumorigenic assay to minimize selection bias. For the 3D multi-spheroid model used to evaluate CSC-mediated anti-cancer drug responses, high-content confocal imaging was performed in live imaging mode at 37 °C and 5% CO_2. To optimize the concentration of Calcein Blue AM, Zombie NIR™ was used to verify its specific labeling of viable cells. This was done by adding Zombie NIR™-stained, dead biosensor-containing cells to a 3D plate of healthy biosensor-containing spheroids, followed by the addition of Calcein Blue AM to label the viable cells.

Image analysis, data processing, and calculation

All image analyses were performed using the Columbus Image Data Storage and Analysis System version 2.9.1 (PerkinElmer). For 3D image analysis, all planes of different z-planes from the confocal images were combined into one maximum projection image, where a pixel with maximum intensity stands for the whole stacking. The maximum projection images were analyzed using the pipelines explained in materials and method "Tumorigenic assay" to "CSC-mediated anti-cancer drug response" sections. The data were then further analyzed, and statistical significance and visualization were performed using R software (http://www.R-project.org/, version 4.3.3). The data and R coding tutorial are available on the website https://kuchikinamthip.github.io/projects/3D-SiSP and GitHub https://github.com/KuchikiNamthip/3D-SiSP.

Applications of 3D multi-spheroid cultures

Tumorigenic assay

To evaluate tumorigenesis, fluorescence-activated cell sorting (FACS)-sorted GFP^{POS} or GFP^{NEG} cells were prepared in 100 µL of complete medium and cultured on the prepared plate (as described in part 3 of the "Materials and methods" section) for 14 days after which all cells were fixed in 4% paraformaldehyde (PFA) for 30 min and stained with 10 µg/mL Hoechst 33342 (Abcam) nuclear staining dye overnight.

The traditional length-based methods were calculated from individual image planes, while all area-based methods (3D-SiSP) were calculated from the maximum projection image. All cells were identified by Hoechst-positive nuclear staining. Thus, the growth of individual clones was detected from the clusters of Hoechst-

positive areas. Area, length, width, and width-to-length were measured from all Hoechst-positive objects (as described in part 5 of the "Materials and methods" section).

For defining spheroid morphology, the spherical shape was defined by a width-to-length ratio between 0.8 and 1.2. Therefore, other objects outside the defined range were considered non-spherical shapes.

For spheroid count, the Hoechst-positive object was determined to be spheroid with cut-offs by area (7853.98 μm^2) or length (100 µm), and then the number of spheroids was counted from each seeding density.

Differentiation status

To evaluate the differentiation status of the spheroids, the experimental method was performed as described in part 6.1 of the "Materials and methods" section. The GFP intensities were quantified from the area of each Hoechst-positive object from the GFP^{POS} group cultured for 14 days. The differentiation status of each spheroid was determined by comparing the GFP intensity of the mCMV-forming spheroid as a background control. In this analysis, we accepted a 10% false positive rate, meaning that spheroids with GFP intensities higher than the highest 10% of the mCMV-forming spheroid intensities were classified as undifferentiated spheroids, while those lower than that cut-off were classified as differentiated spheroids. A step-by-step pseudo-code written in R language is provided as a tutorial for the implementation of this method.

CSC-mediated anti-cancer drug response

Biosensor-containing TFK-1 cells were seeded at 4000 cells in 80 µL of complete medium and cultured on the prepared plate (as described in part 3 of the "Materials and methods" section). The culture was incubated for 3 days to generate 3D multi-spheroids. Next, different concentrations of chemotherapeutics including 5-FU (Selleckchem, #S1209) and gemcitabine (Selleckchem, #S1714) were prepared in 20 µL complete medium containing 0.5% dimethyl sulfoxide (DMSO) and added to the 3D multi-spheroid cultures. Thus, the spheroids treated with 0.5% DMSO were used as vehicle control. After 5 days of treatment, spheroids were stained with 10 µM Calcein Blue AM, a viability dye. A high-content confocal imaging was captured in live mode and between 10 and 70 min after adding Calcein Blue AM. For cytotoxicity evaluation of the anti-cancer drugs, the viable spheroids were identified by Calcein Blue AM, a viability dye. The summation of the Calcein Blue AM-positive area was represented for the cell viability in each drug concentration (CA_{tx}). The summation of the Calcein Blue AM-positive area of each treatment concentration was divided by its vehicle control (CA_{ctrl}) for normalization purposes and represented as 'spheroid viability index (SVI)'.

$$SVI = \frac{\sum CA_{tx}}{\sum CA_{ctrl}}$$

For CSC content under treatment effect, only viable spheroids were included. The 'CSC index' was calculated by the median spheroids' GFP intensity of each spheroid from each drug concentration (GFP_{tx}) normalized with the median spheroids' GFP intensity of the vehicle control (GFP_{ctrl}). The step-by-step pseudo-code written in R language was provided as a tutorial.

$$CSC = \frac{Median\,(GFP_{tx})}{Median\,(GFP_{ctrl})}$$

To compare the CSC index among the anti-cancer drugs, the overlapping SVIs across all drugs were used to define the SVI range. From a defined range of SVI, the trapezoidal rule was used to determine the area under the curve of the CSC index of each drug ($AUC(CSC)_{tx}$). The AUC of CSC indices was expressed as "normalized CSC index's $AUC(CSC_{l\text{-}h})$" after being normalized by the CSC index's AUC of the vehicle control ($AUC(CSC)_{ctrl}$), where l is the lowest SVI and h is the highest SVI. The step-by-step pseudo-code written in R language was provided as a tutorial.

$$CSC_{l-h} = \frac{AUC\,(CSC)_{tx}}{AUC\,(CSC)_{ctrl}}$$

Statistical analysis

All graphs and statistical significance were determined and created with R (http://www.R-project.org/, version 4.3.3). To compare two independent groups, statistical significance was determined using either a two-sided Wilcoxon rank-sum test or a t-test, depending on the data distribution. Correlation analyses were performed using either Pearson or Spearman correlation, according to whether the relationship was linear or non-linear, respectively. Specific statistical tests were mentioned in figure legends. For all investigations, statistical significance was considered when p value < 0.05.

Data availability

The 3D-SiSP experimental protocols for evaluating in vitro tumorigenicity and CSC-mediated anti-cancer drug response were published on protocol.io (https://www.protocols.io/private/ECE27AC5049811EFBE540A58A9FEAC02). The step-by-step pseudo-code written in R language was provided for 5 tutorials below are available on the website https://kuchikinamthip.github.io/projects/3D-SiSP and GitHub https://github.com/KuchikiNamthip/3D-SiSP, please note that the protocol.io, website, and GitHub repository will be publicly online after peer-reviewing. (1) Evaluating the in vitro tumorigenicity of CSC candidate using the 3D multi-spheroid model by determining spheroid number using 3D-SiSP analytical method. (2) Evaluating the in vitro tumorigenicity of

CSC candidate using the 3D multi-spheroid model by determining object area using 3D-SiSP analytical method. (3) Investigating the relationship between spheroid size and their differentiation status for the 3D multi-spheroid model using 3D-SiSP analytical method. (4) Evaluating CSC content and cytotoxicity under anti-cancer drug treatments for the 3D multi-spheroid model using 3D-SiSP analytical method. (5) Comparing CSC content among cytotoxic drugs across a range of spheroid viability index.

Received: 28 February 2025; Accepted: 13 August 2025
Published online: 26 August 2025

References

1. Jensen, C. & Teng, Y. Is it time to start transitioning from 2D to 3D cell culture?. *Front. Mol. Biosci.* **7**, 33. https://doi.org/10.3389/fmolb.2020.00033 (2020).
2. Liu, Y. et al. Patient-derived xenograft models in cancer therapy: Technologies and applications. *Signal Transduct. Target. Ther.* **8**, 160. https://doi.org/10.1038/s41392-023-01419-2 (2023).
3. Flobak, A., Skanland, S. S., Hovig, E., Tasken, K. & Russnes, H. G. Functional precision cancer medicine: Drug sensitivity screening enabled by cell culture models. *Trends Pharmacol. Sci.* **43**, 973–985. https://doi.org/10.1016/j.tips.2022.08.009 (2022).
4. Loh, J. J. & Ma, S. Hallmarks of cancer stemness. *Cell Stem Cell* **31**, 617–639. https://doi.org/10.1016/j.stem.2024.04.004 (2024).
5. Mitrakas, A. G. et al. Applications and advances of multicellular tumor spheroids: Challenges in their development and analysis. *Int. J. Mol. Sci.* **24**, 6949. https://doi.org/10.3390/ijms24086949 (2023).
6. Langhans, S. A. Three-dimensional in vitro cell culture models in drug discovery and drug repositioning. *Front. Pharmacol.* **9**, 6. https://doi.org/10.3389/fphar.2018.00006 (2018).
7. Han, S. J., Kwon, S. & Kim, K. S. Challenges of applying multicellular tumor spheroids in preclinical phase. *Cancer Cell Int.* **21**, 152. https://doi.org/10.1186/s12935-021-01853-8 (2021).
8. Lombardo, Y., de Giorgio, A., Coombes, C. R., Stebbing, J. & Castellano, L. Mammosphere formation assay from human breast cancer tissues and cell lines. *J. Vis. Exp.* https://doi.org/10.3791/52671 (2015).
9. Smart, C. E. et al. In vitro analysis of breast cancer cell line tumourspheres and primary human breast epithelia mammospheres demonstrates inter- and intrasphere heterogeneity. *PLoS ONE* **8**, e64388. https://doi.org/10.1371/journal.pone.0064388 (2013).
10. Mittler, F. et al. High-content monitoring of drug effects in a 3D spheroid model. *Front. Oncol.* **7**, 293. https://doi.org/10.3389/fonc.2017.00293 (2017).
11. Zanoni, M. et al. 3D tumor spheroid models for in vitro therapeutic screening: A systematic approach to enhance the biological relevance of data obtained. *Sci. Rep.* **6**, 19103. https://doi.org/10.1038/srep19103 (2016).
12. Xu, H., Jiao, D., Liu, A. & Wu, K. Tumor organoids: Applications in cancer modeling and potentials in precision medicine. *J. Hematol. Oncol.* **15**, 58. https://doi.org/10.1186/s13045-022-01278-4 (2022).
13. Senrung, A. et al. 3D tumor spheroids: Morphological alterations a yardstick to anti-cancer drug response. *In Vitro Models* **2**, 219–248. https://doi.org/10.1007/s44164-023-00059-8 (2023).
14. Johnson, S., Chen, H. & Lo, P. K. In vitro tumorsphere formation assays. *Bio Protocol* **3**, e325. https://doi.org/10.21769/bioprotoc.325 (2013).
15. Mertens, S. et al. Drug-repurposing screen on patient-derived organoids identifies therapy-induced vulnerability in KRAS-mutant colon cancer. *Cell Rep.* **42**, 112324. https://doi.org/10.1016/j.celrep.2023.112324 (2023).
16. Hong, X., Chedid, K. & Kalkanis, S. N. Glioblastoma cell line-derived spheres in serum-containing medium versus serum-free medium: A comparison of cancer stem cell properties. *Int. J. Oncol.* **41**, 1693–1700. https://doi.org/10.3892/ijo.2012.1592 (2012).
17. Lee, C. H., Yu, C. C., Wang, B. Y. & Chang, W. W. Tumorsphere as an effective in vitro platform for screening anti-cancer stem cell drugs. *Oncotarget* **7**, 1215–1226. https://doi.org/10.18632/oncotarget.6261 (2016).
18. Shan, J. et al. Nanog regulates self-renewal of cancer stem cells through the insulin-like growth factor pathway in human hepatocellular carcinoma. *Hepatology* **56**, 1004–1014. https://doi.org/10.1002/hep.25745 (2012).
19. Bhandary, L. et al. Lipid tethering of breast tumor cells reduces cell aggregation during mammosphere formation. *Sci. Rep.* **11**, 3214. https://doi.org/10.1038/s41598-021-81919-9 (2021).
20. Bailey, P. C. et al. Single-cell tracking of breast cancer cells enables prediction of sphere formation from early cell divisions. *iScience* **8**, 29–39. https://doi.org/10.1016/j.isci.2018.08.015 (2018).
21. Maritan, S. M., Lian, E. Y. & Mulligan, L. M. An efficient and flexible cell aggregation method for 3D spheroid production. *J. Vis. Exp.* https://doi.org/10.3791/55544 (2017).
22. Zhu, Z. W. et al. A novel three-dimensional tumorsphere culture system for the efficient and low-cost enrichment of cancer stem cells with natural polymers. *Exp. Ther. Med.* **15**, 85–92. https://doi.org/10.3892/etm.2017.5419 (2018).
23. Tang, B. et al. A flexible reporter system for direct observation and isolation of cancer stem cells. *Stem Cell Rep.* **4**, 155–169. https://doi.org/10.1016/j.stemcr.2014.11.002 (2015).
24. Huang, Y. et al. Optical coherence tomography detects necrotic regions and volumetrically quantifies multicellular tumor spheroids. *Cancer Res.* **77**, 6011–6020. https://doi.org/10.1158/0008-5472.CAN-17-0821 (2017).
25. Kongtanawanich, K. et al. A live single-cell reporter system reveals drug-induced plasticity of a cancer stem cell-like population in cholangiocarcinoma. *Sci. Rep.* **14**, 22619. https://doi.org/10.1038/s41598-024-73581-8 (2024).
26. Al-Hajj, M., Wicha, M. S., Benito-Hernandez, A., Morrison, S. J. & Clarke, M. F. Prospective identification of tumorigenic breast cancer cells. *Proc. Natl. Acad. Sci. U.S.A.* **100**, 3983–3988. https://doi.org/10.1073/pnas.0530291100 (2003).
27. Singh, S. K. et al. Identification of human brain tumour initiating cells. *Nature* **432**, 396–401. https://doi.org/10.1038/nature03128 (2004).
28. O'Brien, C. A., Pollett, A., Gallinger, S. & Dick, J. E. A human colon cancer cell capable of initiating tumour growth in immunodeficient mice. *Nature* **445**, 106–110. https://doi.org/10.1038/nature05372 (2007).
29. Velletri, T. et al. Single cell-derived spheroids capture the self-renewing subpopulations of metastatic ovarian cancer. *Cell Death Differ.* **29**, 614–626. https://doi.org/10.1038/s41418-021-00878-w (2022).
30. Arima, Y., Nobusue, H. & Saya, H. Targeting of cancer stem cells by differentiation therapy. *Cancer Sci.* **111**, 2689–2695. https://doi.org/10.1111/cas.14504 (2020).
31. De Lara-Peña, L. et al. In *Cancer Stem Cells: Methods and Protocols* (eds Papaccio, F. & Papaccio, G.) 145–161 (Springer, 2024).
32. Cardinale, V. et al. Profiles of cancer stem cell subpopulations in cholangiocarcinomas. *Am. J. Pathol.* **185**, 1724–1739. https://doi.org/10.1016/j.ajpath.2015.02.010 (2015).
33. Kawamoto, M. et al. Combined gemcitabine and metronidazole is a promising therapeutic strategy for cancer stem-like cholangiocarcinoma. *Anticancer Res.* **38**, 2739–2748. https://doi.org/10.21873/anticanres.12516 (2018).
34. Cao, W. et al. LGR5 marks targetable tumor-initiating cells in mouse liver cancer. *Nat. Commun.* **11**, 1961. https://doi.org/10.1038/s41467-020-15846-0 (2020).
35. Prieto-Vila, M., Takahashi, R. U., Usuba, W., Kohama, I. & Ochiya, T. Drug resistance driven by cancer stem cells and their niche. *Int. J. Mol. Sci.* **18**, 2574. https://doi.org/10.3390/ijms18122574 (2017).
36. Gupta, P. B., Pastushenko, I., Skibinski, A., Blanpain, C. & Kuperwasser, C. Phenotypic plasticity: Driver of cancer initiation, progression, and therapy resistance. *Cell Stem Cell* **24**, 65–78. https://doi.org/10.1016/j.stem.2018.11.011 (2019).

37. Dogan, E. et al. Cancer stem cells in tumor modeling: Challenges and future directions. *Adv. Nanobiomed. Res.* **1**, 2100017. https://doi.org/10.1002/anbr.202100017 (2021).
38. Atat, O. E. et al. 3D modeling in cancer studies. *Hum. Cell* **35**, 23–36. https://doi.org/10.1007/s13577-021-00642-9 (2022).
39. Ryu, N. E., Lee, S. H. & Park, H. Spheroid culture system methods and applications for mesenchymal stem cells. *Cells* **8**, 1620. https://doi.org/10.3390/cells8121620 (2019).
40. Ishiguro, T. et al. Tumor-derived spheroids: Relevance to cancer stem cells and clinical applications. *Cancer Sci.* **108**, 283–289. https://doi.org/10.1111/cas.13155 (2017).
41. Badr-Eldin, S. M., Aldawsari, H. M., Kotta, S., Deb, P. K. & Venugopala, K. N. Three-dimensional in vitro cell culture models for efficient drug discovery: Progress so far and future prospects. *Pharmaceuticals (Basel)* **15**, 926. https://doi.org/10.3390/ph15080926 (2022).
42. Ozkan, H., Ozturk, D. G. & Korkmaz, G. Transcriptional factor repertoire of breast cancer in 3D cell culture models. *Cancers (Basel)* **14**, 1023. https://doi.org/10.3390/cancers14041023 (2022).
43. Li, P. et al. Selective single-cell expansion on a microfluidic chip for studying heterogeneity of glioma stem cells. *Anal. Chem.* **94**, 3245–3253. https://doi.org/10.1021/acs.analchem.1c04959 (2022).
44. Rajcevic, U. et al. Colorectal cancer derived organotypic spheroids maintain essential tissue characteristics but adapt their metabolism in culture. *Proteome Sci.* **12**, 39. https://doi.org/10.1186/1477-5956-12-39 (2014).
45. Lotsberg, M. L. et al. Intrinsic differences in spatiotemporal organization and stromal cell interactions between isogenic lung cancer cells of epithelial and mesenchymal phenotypes revealed by high-dimensional single-cell analysis of heterotypic 3D spheroid models. *Front. Oncol.* **12**, 818437. https://doi.org/10.3389/fonc.2022.818437 (2022).
46. Nielsen, B. S. et al. Architectural organization and molecular profiling of 3D cancer heterospheroids and their application in drug testing. *Front. Oncol.* **14**, 1386097. https://doi.org/10.3389/fonc.2024.1386097 (2024).
47. Borten, M. A., Bajikar, S. S., Sasaki, N., Clevers, H. & Janes, K. A. Automated brightfield morphometry of 3D organoid populations by OrganoSeg. *Sci. Rep.* **8**, 5319. https://doi.org/10.1038/s41598-017-18815-8 (2018).
48. Humphries, A. et al. Lineage tracing reveals multipotent stem cells maintain human adenomas and the pattern of clonal expansion in tumor evolution. *Proc. Natl. Acad. Sci. U.S.A.* **110**, E2490-2499. https://doi.org/10.1073/pnas.1220353110 (2013).
49. Greaves, M. & Maley, C. C. Clonal evolution in cancer. *Nature* **481**, 306–313. https://doi.org/10.1038/nature10762 (2012).
50. Kalla, J., Pfneissl, J., Mair, T., Tran, L. & Egger, G. A systematic review on the culture methods and applications of 3D tumoroids for cancer research and personalized medicine. *Cell Oncol. (Dordr.)* https://doi.org/10.1007/s13402-024-00960-8 (2024).
51. Jamnongsong, S. et al. Comprehensive drug response profiling and pan-omic analysis identified therapeutic candidates and prognostic biomarkers for Asian cholangiocarcinoma. *iScience* **25**, 105182. https://doi.org/10.1016/j.isci.2022.105182 (2022).

Acknowledgements

The project is funded by National Research Council of Thailand (NRCT) (N41A640162 and N42A670195) and The Foundation for Cancer Care Siriraj Hospital. K.K. was supported by Chulabhorn Foundation and the Royal Golden Jubilee Ph.D. Scholarship Program (RGJ-PHD) (Grant No. PHD/0060/2561) under Thailand Research Fund (TRF) and NRCT. M.W. is supported by Chalermphrakiat Grant, Faculty of Medicine Siriraj Hospital, Mahidol University. S. Ji. is supported by the R.E.D program, Faculty of Medicine, Siriraj Hospital, Mahidol University. We also thank BioRender for the figure preparation. We would like to thank Dr. Somponnat Sampattavanich, Mahidol University for his support and discussion.

Author contributions

Conceptualization, K.K., M.W., and S.Ji.; Performed the experiments, analyzed data, and visualization, K.K.; Coding validation, S.Ja.; Provided critical comments, S.Ja., M.H., M.W., and S.Ji.; Writing-Original Draft, K.K., M.H., M.W., and S.Ji.; Funding Acquisition, S.Ji.; Resources, S.Ji.; All authors have read and approved the final manuscript.

Declarations

Competing interests

The authors declare no competing interests.

Additional information

Correspondence and requests for materials should be addressed to M.W. or S.J.